Short communication

# Electrochemical properties of the soluble reduction products in rechargeable Li/S battery

Yajuan Li [a,*], Hui Zhan [b,**], Suqin Liu [a], Kelong Huang [a], Yunhong Zhou [b]

[a] Institute of Chemistry and Chemical Engineering, Central South University, Changsha 410083, China
[b] Department of Chemistry, Wuhan University, Wuhan 430072, China

## ABSTRACT

In this paper, the electrochemical behavior of the reduction products in solution for Li/S cell is studied by UV–visual spectroscopy and electrochemical impedance spectroscopy (EIS). The results tell that the redox process of the polysulfide intermediate contains five charge-transfer steps in the practical Li/S cell. The formation of final reduction product of $Li_2S$ and the final re-oxidation product of $S_8$ is completely irreversible. The transform between polysulfide and $Li_2S_2$ is electrochemical sluggish. The peaks corresponding to transformation $Li_2S_x \leftrightarrow Li_2S_y$ $(2 < x < y \leq 6)$ are still symmetrical in spite of an increasing polarization with the proceeding of CV scan. While the redox process corresponding to $Li_2S_m \leftrightarrow Li_2S_n$ $(4 < m < n \leq 8)$ is reversible. The dissolution long-chain polysulfide and deposition of short-chain polysulfide contribute mostly to the electrode deterioration even electrode blockage. Therefore, homogeneous mixing element sulfur with conductive components and alleviating the polysulfide dissolution are equally important to improving the active material utilization and rechargeability for rechargeable Li/S battery.

© 2009 Elsevier B.V. All rights reserved.

## 1. Introduction

The rechargeable Li/S battery has almost the highest theoretical specific energy of 2600 W h kg$^{-1}$, assuming complete reaction to the product $Li_2S$, and furthermore, it possesses the advantages of low cost, environmentally benign and high safety characteristics. However, the practical application of the Li/S rechargeable battery has to face some serious problems of low active material utilization and poor rechargeability, due to the insulating nature of sulfur and solid reduction products and the loss of active material in the form of soluble polysulfide reaction products. Many efforts have been devoted to find the solution for above-mentioned problems, and the sulfur-based composites [1,2], functional cathodes [3,4] and suitable electrolyte [5–7] have been developed to achieve the conductivity improvement or alleviate the dissolution loss of the active material. Though many successful examples have been proposed, the present rechargeability of the Li/S cell is still far from the demand of the practical application.

To find the way out, it is necessary to gain some new insights into the electrochemical behavior of the sulfur electrode [8–10]. In this paper, in order to best reflect the intrinsic electrochemical prop-

erty of every product that is formed during the charge/discharge of sulfur electrode, the in situ electrochemical impedance spectroscopy (EIS) was performed on the soluble polysulfide collected from a discharged Li/S coin cell, which can ensure us the investigation without possible interference from the structural change of the electrode. The purpose is to shed more light on the reaction mechanism of rechargeable Li/S cell and thus to explore the effective method for improving its electrochemical property.

## 2. Experimental

The cathode membrane was fabricated with 40 wt.% sublimed sulfur (purity: 99.5%, Aldrich), 40 wt.% acetylene black and 20 wt.% polytetrafluoroethylene (PTFE) binder. It was cut to 0.8 cm$^2$ in size and was pressed on the stainless steel mesh. The cathodes were dried at 70 °C under vacuum for 24 h. The 2016 coin cell consisted of a sulfur cathode (with ∼2.8 mg sulfur) and a lithium foil anode. The lithium foil anode and the sulfur cathode were separated by a Celgard 2300 membrane together with polypropylene fiber felts (it has a thickness of 80 μm, and also has great uptake of liquid electrolyte). It should be pointed out that four pieces of polypropylene fiber felts were used in order to ensure that the polypropylene fiber felts could absorb enough electrolytes in the discharging test for a further investigation. The electrolyte (Ferro Inc.) was 1 M LiN(CF$_3$SO$_2$)$_2$ solution in a mixed solvent of dioxolane (DXL) and dimethoxyethane (DME) (2:1 by weight). The cathode

* Corresponding author. Tel.: +86 731 88879850; fax: +86 731 88879850.
** Corresponding author. Tel.: +86 27 68756931; fax: +86 27 68754067.
E-mail addresses: yajuanlee@163.com (Y. Li), zhanhui3620@126.com (H. Zhan).

with 8 mg sulfur, lithium foil anode and 6 ml electrolyte were sealed in glass bottle to assemble a bulk cell. All cells were assembled in an argon-filled glove box. The discharge test was carried out on Arbin BT2000 at room temperature. The cell was discharged at a constant current rate of $20\,mA\,g^{-1}$, the cutoff voltage was 1.7 V.

After the discharging test, the 2016 coin cell was disassembled in argon-filled glove box, and the polypropylene fiber felts soaked with electrolyte were taken out. We found that they became yellow, which indicates the presence of the polysulfide [11]. Then, these in situ formed polysulfides were subjected to a further study. First, their cyclic voltammograms were collected on a three-electrode cell at room temperature, a carbon electrode (composed of acetylene black and PTFE in 4:1 weight ratio) acted as the working electrode, lithium foil as both the counter and reference electrode. The lithium counter electrode and the working electrode were separated by a fresh celgard 2300 membrane. The sweep rate was $50\,\mu V\,s^{-1}$. AC impedance experiments were also conducted on above three-electrode cell. Impedance data were collected in a frequency range of 1 MHz to 0.01 Hz with the voltage amplitude of 5 mV. The CV and AC impedance experiments were both conducted using Autolab PGSTAT30.

UV–visual spectroscopy was employed to study the soluble species in electrolyte after the bulk cell was discharge to different depth. After the circuit of the bulk cell was open, 0.06 ml electrolyte in the bulk cell was mixed with 6 ml electrolyte 1 M $LiN(CF_3SO_2)_2/DXL + DME$ (2:1 by weight) in an argon-filled glove box. UV–visual spectroscopy of the mixed solutions was measured with UV-2450 (Shimadzu).

## 3. Results and discussion

### 3.1. The phase transformation of sulfur electrode

The first discharge profile of Li/S 2016 coin cell is shown in Fig. 1. In general, a short upper discharge plateau (at about 2.4 V) was followed by a much longer lower plateau (at about 2.05–2.1 V). For better examining the evolution of sulfur electrode, sulfur electrode was tested in the bulk cell (illustrated in the bottom plot within Fig. 1). The first discharge profiles of the bulk cell were compared with that of the coin cell in Fig. 1. We found that the discharge profiles of sulfur electrode differ greatly according to different electrolytic cell design. Sulfur electrode exhibits four discharging plateaus in bulk cell. The first plateau (at about 2.4 V) is short and quite flat, the second one (at about 2.15–2.25 V) is much longer though a little sloping, the shape of the third discharge plateau seems like a convexity, and a small dip is observed between the second and the third discharge plateaus, the last plateau can be barely discerned from the sloping line between 2.1 and 1.7 V. As in our special electrolytic cell, the cell container is made of transparent glass and this greatly favors our observation. Bottom plot in Fig. 1 clearly shows the change occurring in the electrolytic cell at different discharging state. From the photos in Fig. 1, we find that at "B" point where the discharging capacity begins to be delivered, soluble reduction product with a color of yellow begins to be generated (photo B in Fig. 1). The electrolyte becomes dark-golden at "C" point where seems to be the end of the first discharging plateau. In the second discharging plateau, the color of the electrolyte changes from dark-golden at "C" point to olive at "D" point
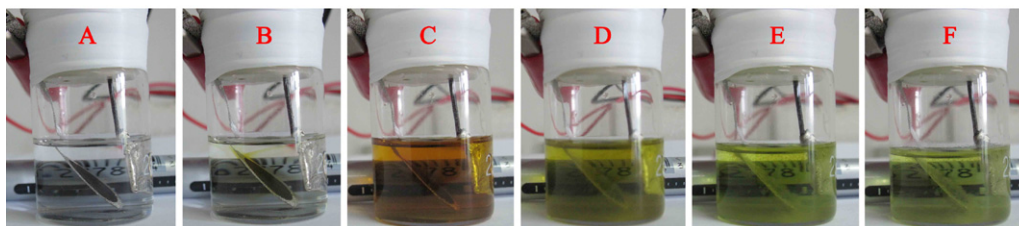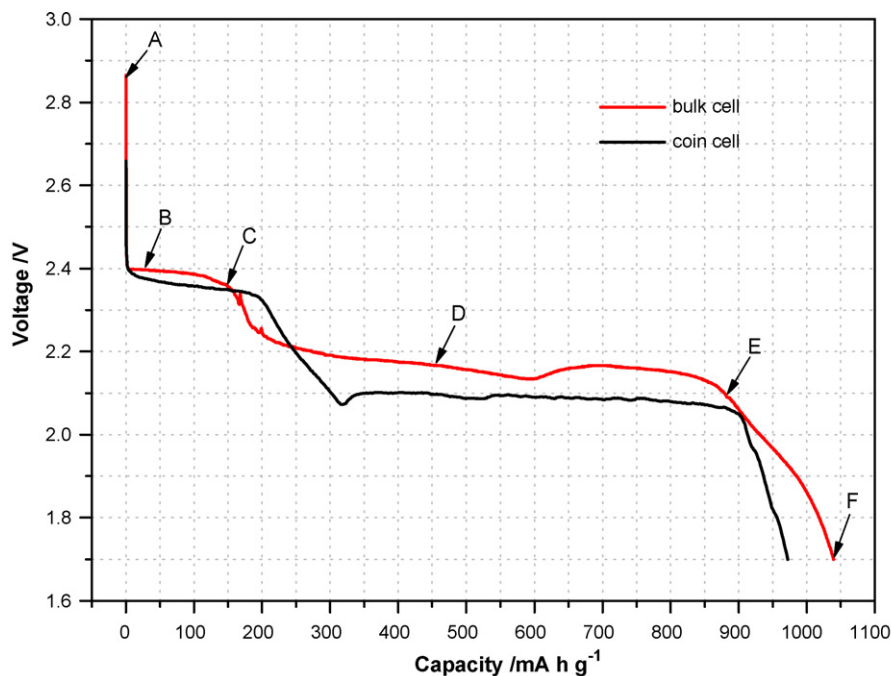


**Fig. 1.** Discharge profiles of lithium sulfur coin cell and bulk cell at $20\,mA\,g^{-1}$ and photos as the bulk cell discharged to varying depth.

accompanied by the formation of precipitation either adhering on the electrode surface or sinking to the bottom of the cell (photo D in Fig. 1). Two conclusions can be reached from these observations. First, the color change probably means the formation of different discharging product. Second, the appearance of precipitation in photo D suggests that the reduction product produced in the second plateau has a low solubility in the electrolyte. In fact, it has been pointed out previously [9] that the solubility of the polysulfide greatly depends on its chain length. So here, we preliminarily speculate that the reduction products in the second plateau are short-chain polysulfides. The photo E and F in Fig. 1 show that the color of the electrolyte becomes green-yellow, but the color in photo F is light, at the same time, the amount of precipitate increases. It suggests that the reduction products of sulfur electrode at the third and fourth plateau are solid. The color of the electrolyte at "F" point also suggests that there are soluble polysulfides in electrolyte even at the end of discharging process, it is one of reason why the active material utilization of sulfur electrode is low.

Fig. 2 compares the UV–visual spectroscopy of soluble reduction products formed at different discharging depth. When the bulk cell is discharge to 2.33 V, four peaks are detected which exhibit max absorbance at 237 nm, 262 nm, 270 nm and 280 nm, as shown in Fig. 2a. Fig. 2b exhibits distinct absorbance in 233–280 nm region, and a shoulder peak appear in the 334 nm. While in Fig. 2c, there are a narrow peak at 250 nm and a broad peak at about 420 nm, the absorbance at about 334 nm decreases comparing with Fig. 2b, but it still stronger than that in Fig. 2a. The peaks at 237 nm, 262 nm, 270 nm and 280 nm are considered to correspond to the to long-chain reduction species. The peak at 250 nm is assigned to short-chain polysulfide. The absorbance at 334 nm and 420 nm correspond to $S_3^{2-}$ and $S_4^{2-}$, respectively according to previous work [8]. The yellow-green color (mixture of blue and yellow) of the electrolyte at "E" and "F" point (photo E and F in Fig. 1) are due to $S_3^{2-}$ (it is a blue species) and $S_4^{2-}$ (it is a yellow species), according to previous work [11]. The olive color (mixture of green-yellow and dark-golden) of the electrolyte at "D" is due to the short-chain polysulfide ($S_3^{2-}$ and $S_4^{2-}$) and the long-chain polysulfide. It should be pointed out that the electrolyte color fades slowly and there is precipitate on the bottom of the bulk cell after the circuit of the bulk cell is open, which is discharged to 2.33 V, while after discharged to 2.16 and 1.7 V, the electrolyte in the bulk cell retains their color under open circuit. The soluble reduction product will be detected by multiple in situ spectroelectrochemical and discussed in another paper.
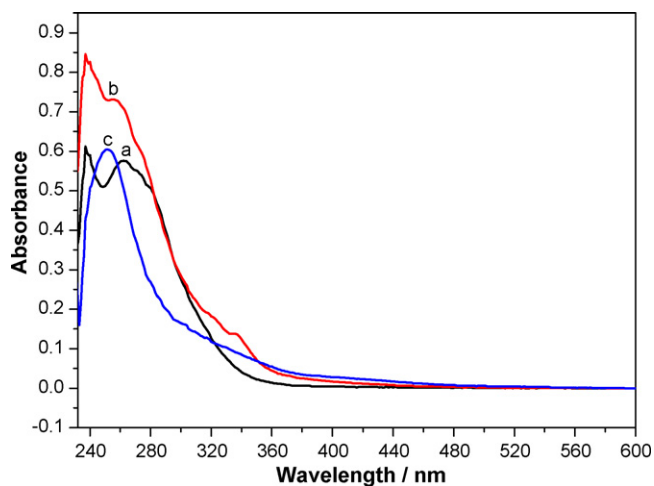
As the electrochemical behavior of sulfur electrode is easily affected by the design of electrolytic cell, in order to best reflect the intrinsic electrochemical property of every product that is formed during the charge/discharge of practical Li/S cell, the soluble polysulfide obtained from coin cell were chosen as our studying object in following EIS study.

### 3.2. Redox behavior of soluble polysulfide between 1.70 and 3.00 V

The cyclic voltammograms of the polysulfide between 1.70 and 3.00 V are shown in Fig. 3a, which exhibit three pair of redox peaks. In the first anodizing started from the open circuit potential (OCP), two oxidation peaks locating at 2.412 and 2.800 V is observed, but in the second scan, the anodic peak at 2.800 V becomes inconspicuous while the other still remains. It seems that the reaction and the related product behind these two peaks differ a lot. To make it clear, impedance diagram was in situ collected at 2.412 and 2.800 V during the first anodic sweep, and the results are shown in Fig. 4. The equivalent circuits and fitting plots of the experimental data were shown in Fig. 4, too. Although many models are possible, these models give a reasonably good fit to the experimental data and make physical sense. At 2.412 V, the polysulfide electrode exhibits one compressed semicircle in the high frequency and a sloping straight line in the low frequency. In its equivalent circuit mode, $R_{ct}$ represents the charge-transfer resistance generated at the carbon electrode/electrolyte interface, the constant phase element ($CPE_{dl}$) is used to replace the double-layer capacitance, the constant phase element ($CPE_1$) relates to liquid-state diffusion of the soluble polysulfide. The component values are shown in Table 1. This oxidation process corresponds to the reaction $Li_2S_m \rightarrow Li_2S_n$ ($4 < m < n \leq 8$) according to above section. At 2.800 V, the obtained impedance spectrum contains two semicircles, one in the high frequency and the other in the low frequency.
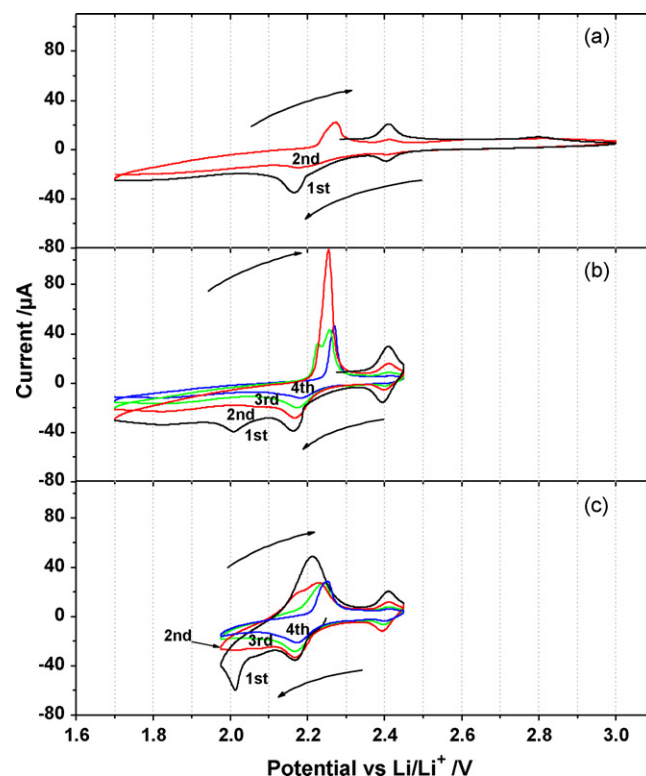


Fig. 2. Spectra obtained after the bulk cell discharged to: (a) 2.33 V, (b) 2.16 V (near the end of the second plateau in Fig. 1) and (c) 1.70 V.



Fig. 3. Cyclic voltammograms of polysulfide (a) between 1.70 and 3.00 V; (b) between 1.70 and 2.45 V; (c) 1.98–2.45 V (scan rate: 50 μV s$^{-1}$).
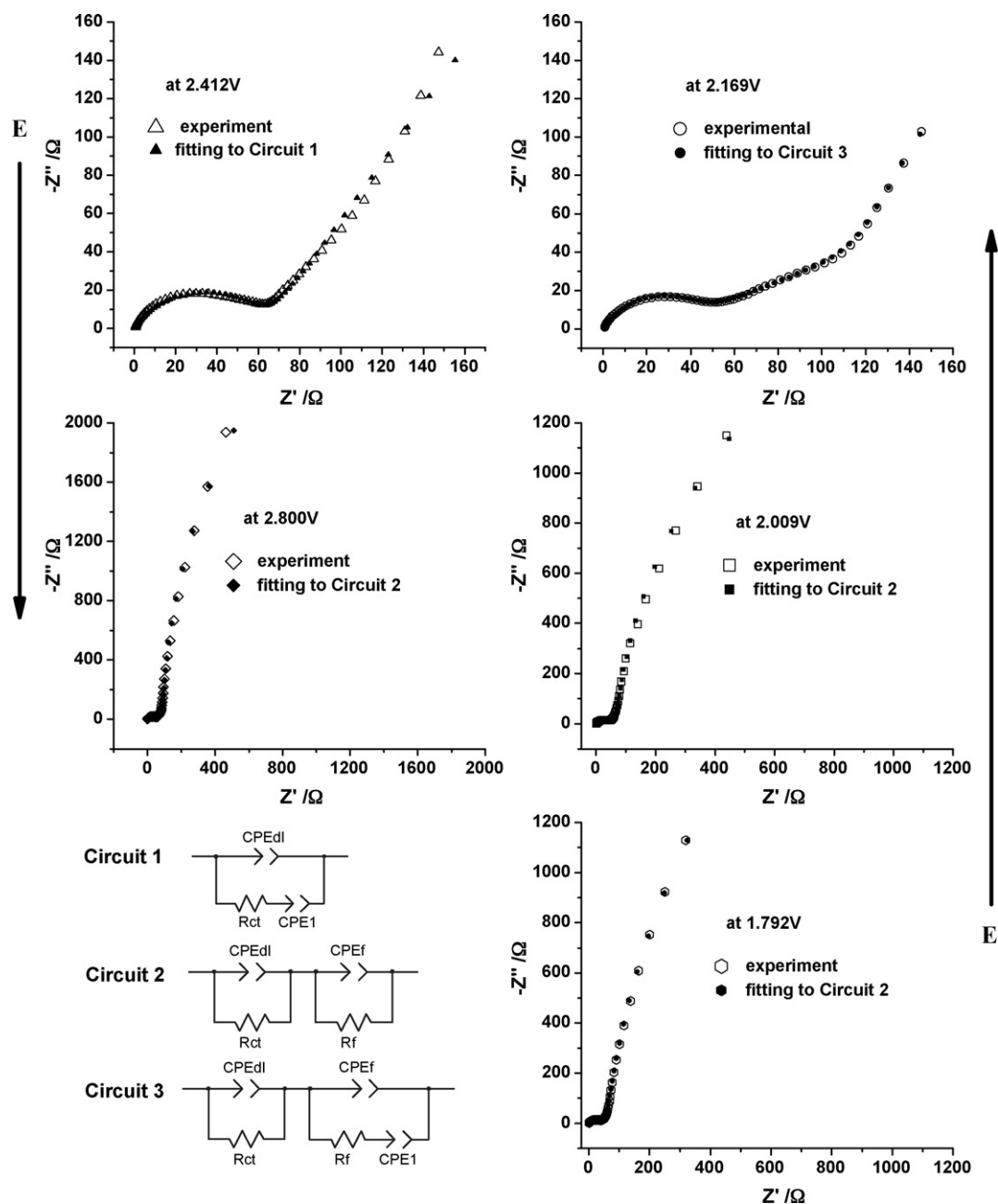
**Fig. 4.** Nyquist plots of the polysulfide electrode at various potentials and equivalent circuit used in fitting the data.

In its equivalent circuit mode, $R_{ct}$ and $CPE_{dl}$ make the same physical sense to the components of the circuit model at 2.412 V. $R_f$ represents the charge-transfer resistance on the surface of the newly formed phase, and $CPE_f$ replaces the double-layer capacitance on the new phase/electrolyte interface. The component values are shown in Table 1 for comparison. The fitting result tells us that the value of $R_f$ is much bigger than that of $R_{ct}$, it may suggest the insulating nature of the new phase. Carefully considering the possible oxidation product of the polysulfide, it can be inferred that the new phase formed at about 2.800 V is likely to be $S_8$, which

**Table 1**
Results of fitting the data in Fig. 4 to the equivalent circuit.

| | $R_{ct}$ ($\Omega$) | $CPE_{dl}$[a] | | $R_f$ (k$\Omega$) | $CPE_f$[a] | | $CPE_1$[a] | |
|---|---|---|---|---|---|---|---|---|
| | | $Y_0$ ($\Omega^{-1}$) $\times 10^{-4}$ | $n$ | | $Y_0$ ($\Omega^{-1}$) $\times 10^{-3}$ | $n$ | $Y_0$ ($\Omega^{-1}$) $\times 10^{-2}$ | $n$ |
| 2.800 V | 78.4 ± 8.6 | 6.11 ± 0.67 | 0.583 ± 0.064 | 15.5 ± 1.7 | 6.99 ± 0.77 | 0.955 ± 0.105 | – | – |
| 2.412 V | 66.5 ± 2.9 | 5.27 ± 0.23 | 0.644 ± 0.028 | – | – | – | 3.40 ± 0.15 | 0.632 ± 0.027 |
| 2.169 V | 57.3 ± 0.5 | 142 ± 1 | 0.668 ± 0.005 | 0.0528 ± 0.0002 | 0.350 ± 0.002 | 0.688 ± 0.004 | 7.90 ± 0.05 | 0.756 ± 0.005 |
| 2.009 V | 71.7 ± 7.2 | 13.5 ± 1.4 | 0.510 ± 0.051 | 4.77 ± 0.48 | 11.2 ± 1.1 | 0.957 ± 0.096 | – | – |
| 1.792 V | 60.2 ± 5.2 | 10.1 ± 0.9 | 0.563 ± 0.049 | 8.32 ± 0.72 | 11.4 ± 1 | 0.942 ± 0.082 | – | – |

[a] The CPE is defined by the impedance relationship $Z = 1/Y_0(i\omega)^{-n}$.

is usually characteristic of the insolubility and electrical insulation.

### 3.3. Redox behavior of soluble polysulfide between 1.70 and 2.45 V

To study the electrochemical behavior free of the interference from the formation of insulating $S_8$, a further CV measurement was conducted between 1.70 and 2.45 V and the result is shown in Fig. 3b. It is interesting to find that four cathodic peaks are observed but only corresponding to two or three anodic ones (the peak at 2.25 V maybe combine two anodizing process). As known, the polysulfide electrode can be electro-reduced to other polysulfide with a shorter-chain and ultimately to $Li_2S$ at full reduction. So, it is reliably believed that the appearance of four cathodic peaks associate to the formation of different reduction product. In other words, these four peaks correspond to four plateaus in Fig. 1. In Fig. 3b, there is obvious change in the peak current, and the cathodic peak at 2.009 V present in the first scan almost becomes indiscernible in the subsequent scan. All these results seem to imply that during the reduction of polysulfide, some low-activity products are formed and this results in the deterioration of the electrode.

To examine the nature of the reduction product, as the polysulfide electrode was linearly scanned toward the cathodic direction from the OCP, the impedance measurement was carried out at 2.169 V, 2.009 V and 1.792 V, corresponding the reduction peak potential in Fig. 3b. The impedance diagrams are presented in Fig. 4. The AC impedance spectrum at different cathode potential differs a lot, their equivalent circuits and fitting plots were shown in Fig. 4, too. The components make the same physical sense as above discussion, and the component values are shown in Table 1. At 2.169 V, it is composed of two semicircles and an inclined line. The coexistence of CPE1 and $R_f$ suggested that both the liquid-state diffusion and formation of new phase were involved. So, here, the appearance of "$R_f$" relates to the partially precipitates of less soluble polysulfide $S_4^{2-}$ and $S_3^{2-}$ on the carbon electrode. While, there is no CPE1 in the equivalent circuits for the impedance spectra collected at 2.009 and 1.792 V, at these potentials, the liquid phase diffusion becomes insignificant because of the formation of insoluble and insulating phase and that-resulted electrode blockage. The data in Table 1 show that the $R_f$ value increases with the gradually decreased cathode potential. It implies poor conductivity and insolubility phase develops gradually. Considering the possible reduction product of polysulfides, it is believed that polysulfide intermediate $S_4^{2-}$ and $S_3^{2-}$ formed near 2.169 V, the formation of $Li_2S_2$ occurred near 2.009 V and even $Li_2S$ near 1.792 V.

### 3.4. Redox behavior of soluble polysulfide between 1.98 and 2.45 V

From above section, a complete reduction reaction to $Li_2S$ is very difficult to achieve. In fact, this is the main reason why the special capacity of Li/S cell is far below the theoretical capacity ($1675 \, mAh \, g^{-1}$). But it does not necessarily mean that without the formation of $Li_2S$, fast reaction kinetics of the sulfur electrode

can be guaranteed. We further examine the CV behavior of the polysulfide electrode in the potential range of 1.98–2.45 V, and the result is shown in Fig. 3c. Three pairs of redox peaks can be observed. Among them, the redox peaks at 2.412 V/2.393 V show the highest symmetry. Combined with the impedance analysis in above section, it is inferred that this redox process corresponds $Li_2S_m \leftrightarrow Li_2S_n$ ($4 < m < n \leq 8$). The ones at 2.230 V/2.169 V are still symmetrical in spite of an increasing polarization. Also combined with above discussion, this redox couple should mainly represent the transformation $Li_2S_x \leftrightarrow Li_2S_y$ ($2 < x < y \leq 6$). The redox process at 2.170 V/2.009 V correspond the transform between polysulfide and $Li_2S_2$ from above discussion, the great peak separation (about 160 mV) tells that it is electrochemical sluggish. Although the anodic peak shift to negative potential about 40 mV comparing to that in Fig. 3b, with the proceeding of CV scan, the peak current drops quickly. So, in a practical Li/S cell, an improvement on the electrochemical activity of sulfur electrode is necessary to the discharge capacity retention.

## 4. Conclusions

We have demonstrated that the discharge of Li/S cell unavoidably causes the formation of soluble polysulfides in ether-based electrolyte, and the re-oxidation or re-reduction of these polysulfides unavoidably incurs the deposition and aggregation of insulated $S_8$ or short-chain reduction products on the electrode surface, even brings electrode blockage. Therefore, the enhancement of the electronic conductivity of sulfur electrode and inhibition of the dissolution of polysulfide must be carried out at one time for rechargeable Li/S battery.

## References

[1] J.L. Wang, J. Yang, J.Y. Xie, N.X. Xu, Y. Li, Electrochem. Commun. 4 (2002) 499–502.
[2] Y.J. Choi, Y.D. Chung, C.Y. Baek, K.W. Kim, H.J. Ahn, J.H. Ahn, J. Power Sources 184 (2008) 548–552.
[3] J. Sun, Y. Huang, W. Wang, Z. Yu, A. Wang, K. Yuan, Electrochim. Acta 53 (2008) 7084–7088.
[4] M.-S. Song, S.-C. Han, H.-S. Kim, J.-H. Kim, K.-T. Kim, Y.-M. Kang, H.-J. Ahn, S.X. Dou, J.-Y. Lee, J. Electrochem. Soc. 151 (6) (2004) A791–A795.
[5] L.X. Yuan, J.K. Feng, X.P. Ai, Y.L. Cao, S.L. Chen, H.X. Yang, Electrochem. Commun. 8 (2006) 610–614.
[6] D. Marmorstein, T.H. Yu, K.A. Striebel, F.R. McLarnon, J. Hou, E.J. Cairns, J. Power Sources 89 (2000) 219–226.
[7] H. Akitoshi, O. Takamasa, M. Fuminori, T. Kiyoharu, T. Masahiro, Electrochem. Commun. 5 (2003) 701–705.
[8] D.-H. Han, B.-S. Kim, S.-J. Choi, Y. Jung, J. Kwak, S.-M. Park, J. Electrochem. Soc. 151 (9) (2004) E283–E290.
[9] H. Yamin, J. Penciner, A. Gorenshtain, M. Elam, E. Peled, J. Power Sources 14 (1985) 129–134.
[10] L. Yuan, X. Qiu, L. Chen, W. Zhu, J. Power Sources 187 (2009) 127–132.
[11] S.-I. Tobishima, H. Yamamoto, M. Matsuda, Electrochim. Acta 42 (1997) 1019–1029.